iScience

Article

Design of a fragment crystallizable-engineered tetravalent bispecific antibody targeting programmed cell death-1 and vascular endothelial growth factor with cooperative biological effects

Graphical abstract

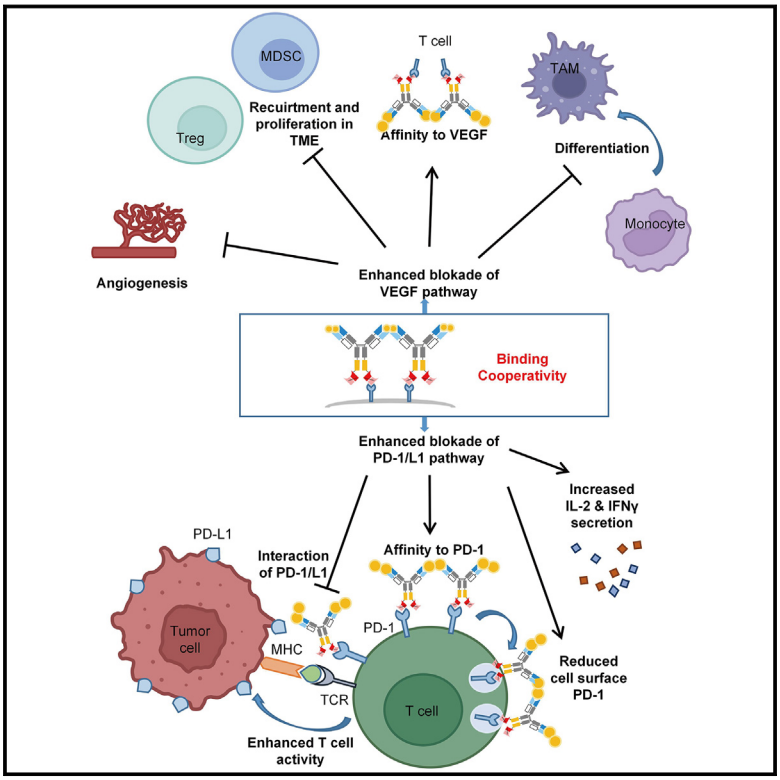

Highlights

- Ivonescimab binds PD-1 and VEGF simultaneously resulting in cooperative binding
- Cooperative binding leads to enhanced potency on blockade of PD-1 and VEGF signaling
- Fc-engineering endows ivonescimab reduced effector function and good safety in the clinic

Authors

Tingting Zhong, Lingzhi Zhang, Zhaoliang Huang, ..., Jing Min, Michelle Xia, Baiyong Li

Correspondence

baiyong.li@akesobio.com

In brief

Therapeutics; Molecular biology; Cancer

Zhong et al., 2025, iScience *28*, 111722
March 21, 2025
https://doi.org/10.1016/j.isci.2024.111722

CellPress

iScience

CellPress
OPEN ACCESS

Article

Design of a fragment crystallizable-engineered tetravalent bispecific antibody targeting programmed cell death-1 and vascular endothelial growth factor with cooperative biological effects

Tingting Zhong,[1] Lingzhi Zhang,[1] Zhaoliang Huang,[1] Xinghua Pang,[1] Chunshan Jin,[1] Wenrong Liu,[1] Juan Du,[1] Wen Yin,[1] Na Chen,[1] Jing Min,[1] Michelle Xia,[2] and Baiyong Li[1,3,*]

[1]Research and Development Department, Akeso Biopharma Inc., No.6 Shennong Road, Torch Development Zone, Zhongshan, Guangdong 528400, China

[2]President's Office, Akeso Biopharma Inc., No.6 Shennong Road, Torch Development Zone, Zhongshan, Guangdong 528400, China

[3]Lead contact

*Correspondence: baiyong.li@akesobio.com

https://doi.org/10.1016/j.isci.2024.111722

SUMMARY

Clinical studies have shown that combination therapy of PD-1 and VEGF antibodies significantly improves clinical benefit over PD-1 antibody alone in certain settings. Ivonescimab, an on-market tetravalent anti-PD-1/VEGF bispecific antibody, was designed to improve efficacy and safety over combo therapy. In this study, the mechanism of action is investigated. In the presence of VEGF, ivonescimab forms soluble complexes with VEGF dimers, leading to the enhanced binding avidity of ivonescimab to PD-1 therefore promoting its increased potency on PD-1/PD-L1-signaling blockade. Likewise, PD-1 binding enhanced ivonescimab binding to VEGF, therefore enhancing VEGF-signaling blockade. Furthermore, ivonescimab treatment demonstrated statistically significant anti-tumor response *in vivo*. Moreover, ivonescimab contains Fc-silencing mutations abrogating FcγRI/IIIa binding and showed significantly reduced effector function *in vitro* which is consistent with the better safety profile of ivonescimab in monkeys and humans. Briefly, ivonescimab displays unique cooperative binding and promotes the increased *in vitro* functional bioactivities with a favorable safety profile.

INTRODUCTION

Blockade of programmed cell death-1 (PD-1)/programmed cell death ligand-1 (PD-L1) is a proven effective immunotherapy in cancer treatment. Intrinsic mechanistic complementation of the immune checkpoint and vascular endothelial growth factor (VEGF) pathways, including VEGF effect on angiogenesis, immune cell infiltration, and dendritic cell maturation, provide a strong rationale for the combination of anti-PD-1/PD-L1 antibodies and anti-VEGF/VEGFR antibodies for cancer therapy.

Combination treatments using anti-PD-1/PD-L1 agents with anti-VEGF therapy have shown enhanced clinical antitumor activities.[1] Such a regimen has become standard of care for hepatocellular carcinoma, yet major side effects caused by angiogenesis inhibition hindered broader use of this approach.[2] For example, adding VEGF antibody treatment to the standard of care for squamous non-small cell lung cancer is known to cause severe hemoptysis and other side effects.[3]

Consequently, a first-in-class anti-PD-1/VEGF bispecific antibody ivonescimab (AK112/SMT112) was designed to inhibit PD-1-mediated immunosuppression and simultaneously block VEGF signaling in the tumor microenvironment (TME). Ivonescimab was designed to enable the simultaneous binding of the PD-1 and VEGF targets. In our pre-clinical studies, the tetravalent structure of ivonescimab allowed the formation of large complexes with dimeric VEGF, resulting in improved avidity to PD-1 and an increase in functional valency and potency. PD-1 binding to ivonescimab also enhanced its binding affinity to VEGF and the enhanced potency in depleting VEGF. This mutual cooperativity elicited the potent anti-tumor efficacy in mice. Additionally, the fragment crystallizable (Fc) engineering of ivonescimab eliminated its Fc effector functions including antibody-dependent cell-mediated cytotoxicity (ADCC), complement-dependent cytotoxicity (CDC), antibody-dependent cell phagocytosis (ADCP), antibody-dependent cytokine release (ADCR) and cytokine release syndrome (CRS), which may contribute to fewer immune-related adverse events (irAEs). These features of ivonescimab are consistent with safety and efficacy improvement over historical PD-1 and VEGF antibody combination results in the clinic.[4–6]

RESULTS

Ivonescimab binds to human programmed cell death-1 and vascular endothelial growth factor, blocks downstream signaling, and inhibits functional activities

Ivonescimab was designed as a tetravalent and symmetric bispecific antibody that targets both PD-1 and VEGF, constructed using Akeso Biopharma PD-1 antibody penpulimab (AK105)

Table 1. Antigen binding activity of ivonescimab to PD-1 and VEGF

	EC50 (nM) of antigen binding activity			KD (M) of antigen binding affinity	
	ELISA[a]		FACS[b]	Fortebio[c]	
Antibody	PD-1	VEGF	293T-PD-1 cells	PD-1	VEGF
Ivonescimab	0.060	0.036	3.49	2.46E-10	3.30E-10
Bevacizumab	NA	0.035	NA	NA	6.64E-10
Nivolumab	0.044	NA	2.10	2.48E-10	NA

NA, not applicable.
[a]Fusion protein of mouse Fc with human PD-1 extracellular domain or 6× histidine-tagged VEGF protein was fixed onto the plates in the assays.
[b]293T cells transfected with human PD-1 (293T-PD-1 cells) were used as target cells in the assay.
[c]Biotinylated fusion protein of human Fc with human PD-1 extracellular domain or 6× histidine-tagged VEGF protein was immobilized onto the sensor in the assays.

and anti-VEGF antibody bevacizumab. To characterize the binding activities of ivonescimab, the binding kinetics of ivonescimab to recombinant human PD-1 and VEGF were first determined by Fortebio Octet analysis. The K_D for the binding of ivonescimab to PD-1 was 2.46×10^{-10} M and 3.3×10^{-10} M to VEGF, comparable to that of nivolumab and bevacizumab, respectively. In addition, the antigen binding activity of ivonescimab to PD-1 and VEGF were assessed by ELISA. The binding EC_{50} of ivonescimab to plate-coated PD-1 and VEGF were 0.06 nM and 0.036 nM, respectively. Ivonescimab also showed high binding activity to PD-1 overexpressed in 293T cells. Above all, we show that ivonescimab binds to both PD-1 and VEGF with high affinity (Table 1). Moreover, the binding activity was further detected using Fortebio Octet analysis by adding PD-1 and VEGF sequentially, and the result demonstrated that ivonescimab could concurrently bind to human PD-1 and VEGF (Figures 1A and 1B). In a competitive ELISA assay, ivonescimab showed high potency in the blockade of both PD-1/PD-L1 and VEGF/VEGFR interactions (Figures 1C and 1E). The bioactivity of ivonescimab to block PD-1 and VEGF signaling pathways was further determined in nuclear factor of activated T cells (NFAT) luciferase reporter assays. As shown in Figures 1D and 1F, ivonescimab efficiently blocked the PD-1 signaling (IC_{50} = 22.54 nM) and VEGF signaling (IC_{50} = 3.13 nM), comparable to the parental antibody penpulimab and bevacizumab. As a highly specific pro-vascular endothelial cell growth factor, VEGF has been shown to promote endothelial cell survival and proliferation as well as play a crucial physiological role in angiogenesis, maintenance, and the enhancement of vascular permeability.[1,7] Therefore, we investigated the inhibitory properties of ivonescimab to VEGF-mediated effects on human umbilical vein endothelial cells (HUVECs). The result showed that ivonescimab has a significantly strong inhibitory effect on the VEGF-induced HUVEC proliferation (Figure 1F). Altogether, these data suggest that ivonescimab simultaneously binds to human PD-1 and VEGF with high affinity and has high potency on PD-1 and VEGF signaling pathway blockade.

Ivonescimab forms soluble complexes with vascular endothelial growth factor, resulting in cooperative binding to its targets and enhanced blockade of both programmed cell death-1/programmed cell death ligand-1 and vascular endothelial growth factor/VEGFR signaling

VEGF is secreted as a functional dimer in which the two monomers are linked together by two inter-subunit disulfide bridges. Bevacizumab was reported to form large complexes with dimeric VEGF.[8,9] To determine whether ivonescimab can do the same, VEGF was mixed and incubated with ivonescimab in solution at different molar ratios (1:8, 1:4, 1:2, 2:1, 4:1, and 8:1), and the formation of ivonescimab-VEGF complexes was detected by size-exclusion high-pressure liquid chromatography (SEC-HPLC). As shown in Figures 2 and S1, ivonescimab was found to form a heterogeneous mixture of multimeric complexes in the presence of VEGF at all different ratios.

Since VEGF is highly enriched in the tumor environment and can form a protein complex with ivonescimab, we speculated that whether the ivonescimab-VEGF complex could mediate its binding avidity to its target. First of all, to determine if VEGF could enhance the avidity of ivonescimab to PD-1, the binding activity of ivonescimab to PD-1 in the presence or absence of VEGF was evaluated by Fortebio Octet analysis and flow cytometry. As shown in Figures 3A and 3B, antigen binding avidity of ivonescimab to PD-1 was significantly enhanced in the presence of VEGF. The binding kinetic results showed a more than 18-fold increase in K_D, mainly driven by the slower dissociation rate (k_{dis}). In addition, dramatically increased the binding of ivonescimab to PD-1 transfected Jurkat cells was observed in the presence of VEGF, whereas anti-PD-1 antibody penpulimab did not show enhanced binding in the presence of VEGF (Figures S2 and 3C). It has been reported that anti-PD-1 antibodies could induce PD-1 internalization, thereby maximize T cell activation. Notably, the presence of VEGF obviously augmented the reduced cell-surface PD-1 expression by ivonescimab in PD-1-expressing Jurkat cells by FACS (Figure 3D). Meanwhile, the internalization properties of ivonescimab and parental antibody penpulimab into 293T-PD-1 cells (human PD-1 overexpressing HEK293T cells) in the presence of VEGF or not were monitored by microscopy. The results showed that ivonescimab in the presence of VEGF rapidly internalized compare to ivonescimab alone whereas penpulimab in the presence of VEGF or not both showed moderate internalization (Figure S3). As a result, in the presence of VEGF, ivonescimab demonstrated the enhanced blockade of PD-1/PD-L1 signaling in a luciferase reporter cell assay (IC_{50} = 3.29 nM) compared to ivonescimab alone (IC_{50} = 17.16 nM) (Figure 3E). Blockade of PD-1 pathways leads to the activation of T cells, evidenced by the enhanced cytokines secretion (IFN-γ, IL-2) by human primary T cells.[10] The ability of ivonescimab to promote T cell responses with or without VEGF was examined in an assay system composed of human PBMCs and Raji-PD-L1 cells (human PD-L1 overexpressing Raji cells). As shown in Figures 3F and 3G, both IFN-γ and IL-2 levels increased in a dose-dependent manner after ivonescimab or penpulimab treatment. Compared with ivonescimab alone, ivonescimab plus VEGF showed increased activity in promoting IFN-γ and IL-2 secretion, while penpulimab plus VEGF did not

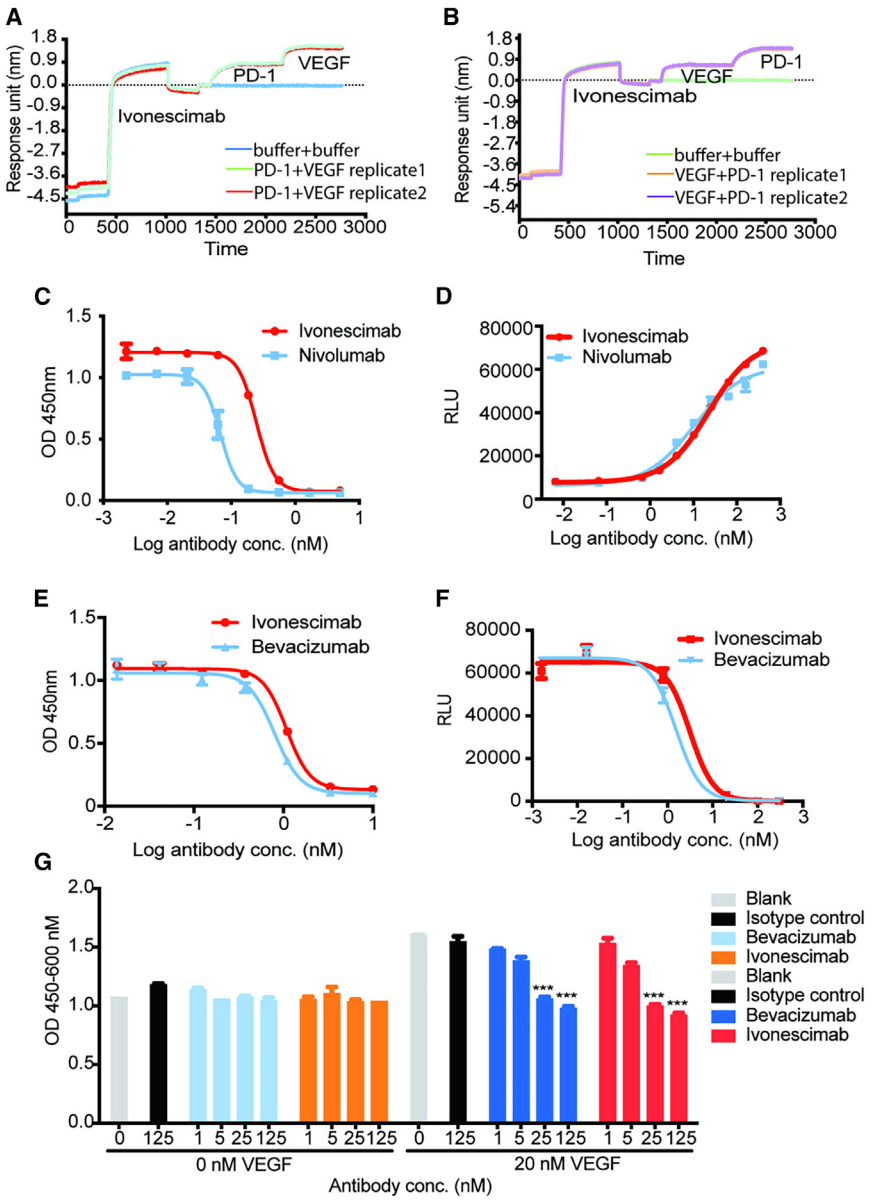

Figure 1. Ivonescimab blocks PD-1/PD-L1 or VEGF/VEGFR signaling and inhibits VEGF-induced HUVECs proliferation

(A and B) The binding kinetics of ivonescimab to PD-1 and VEGF simultaneously were determined by Fortebio Octet. Ivonescimab was fixed onto the AR2G sensor for 600 s and sequential binding to human PD-1 (PD-1-hFc, 300 s) and VEGF (VEGF-His, 300 s) or in reverse order was performed in two replicates and measured. Buffer only were used as controls.

(C) Inhibition of human PD-L1-mFc binding to human PD1-hFc by ivonescimab and nivolumab were determined by ELISA.

(D) Ivonescimab blocks PD-1/PD-L1 signaling. Luminescence signals in the co-culture of PD-L1 aAPC/CHO-K1 cells and PD-1 effector cells were detected by Steady-Glo Luciferase assay. RLU, relative light units.

(E) Inhibition of human VEGFR2-mFc-Bio binding to human VEGF-His by ivonescimab and bevacizumab was determined by ELISA.

(F) Ivonescimab blocks VEGF/VEGFR signaling in VEGF-mediated reporter assay. Luminescence signals in the 293T-KDR-NFAT-LUC cells treated with VEGF alone or VEGF with different concentrations of antibodies as indicated were assessed by Steady-Glo Luciferase assay.

(G) Different concentrations of antibodies added with or without VEGF (20 nM) were co-cultured with the HUVEC cells for 3 days. The viable cells were quantified in CCK8 assay. Compared with the isotype control+20 nM VEGF, ***$p < 0.001$.

elicit this ability when compared with pennulimab alone. These data demonstrated that VEGF promotes the cooperative binding of ivonescimab to PD-1 and, therefore, augmented blockade of PD-1/PD-L1 signaling and enhanced T cell activation.

Since the tetravalent structure of ivonescimab allowed the formation of ivonescimab-VEGF complexes and enhanced its binding to PD-1 and its potency to block PD-1 signaling, we next sought to determine if PD-1 could enhance the avidity of ivonescimab to VEGF. The binding activity of ivonescimab with VEGF was evaluated by Fortebio Octet analysis in the presence of PD-1-hFc. As shown in Figures 4A and 4B, the binding kinetic results showed a more than 4-fold increase of affinity to VEGF in the presence of PD-1-hFc, while the binding affinity of bevacizumab to VEGF was not altered (Figure S2). Moreover, to mimic the realistic tumor microenvironment, we incubated antibodies with PD-1-His-Biotin coated beads and then detected the unbound free VEGF in the supernatant and further used the reporter assay to evaluate the VEGF signaling triggered by free VEGF. As shown in Figure 4C, ivonescimab in the condition with PD-1 increased the depletion of free VEGF in the solution compared to no PD-1 condition (Figure 4C). Consequently, a significantly enhanced VEGF/VEGFR blockade was observed by soluble VEGF in the condition of ivonescimab with PD-1 compared to ivonescimab alone, while bevacizumab had similar effects on VEGF signaling with or without PD-1 (Figure 4D). These results suggest that PD-1 enhances the cooperative binding of ivonescimab to VEGF and, therefore, confers it with better potency in blocking VEGF signaling.

Ivonescimab demonstrates robust anti-tumor activity in mouse models

Next, the anti-tumor activity of ivonescimab monotherapy was evaluated and compared with that of bevacizumab in PBMC humanized SCID/Beige mice with subcutaneous HCC827 xenograft tumors. The treatment of ivonescimab at 1.4 mg/kg or 14 mg/kg resulted in strong tumor growth inhibition in a dose-dependent fashion. The anti-tumor effect was greater than bevacizumab at the equivalent molarity doses of 1 mg/kg or

10 mg/kg (Figures 5A and 5B). All mice survived until the end of the experiment (Figure S4), and we also did not observe noticeable changes in body weight in any of these groups (Figure 5C). Since synergistic anti-tumor activity can be achieved by combination immunotherapies that target different or non-overlapping biological pathways, the combinatorial anti-tumor activity of ivonescimab with two other proprietary anti-tumor drugs was also investigated in mouse tumor models. AK117 is an anti-CD47 antibody and AK119 is an anti-CD73 antibody that is developed by Akeso Biopharma. Notably, when compared with the monotherapy of ivonescimab or AK117 alone, the combination treatment of ivonescimab and AK117 led to the significantly increased tumor inhibition in the PBMC-humanized SCID/Beige mice model with subcutaneous MDA-MB-231 xenograft tumors (Figure 5D). Moreover, the combination of ivonescimab with AK119 also inhibited tumor growth to a greater extent than the monotherapy in C57BL/6-hPD-1/hPD-L1/hCD73 transgenic mice which bearing humanized PD-L1/CD73 MC38 tumors (Figure 5E). These data provide strong evidence that ivonescimab has promising *in vivo* anti-tumor activity both as monotherapy and combination therapy.

Fc-null engineering of ivonescimab abrogates its interactions with FcγRs and reduces the fragment crystallizable-mediated antibody-dependent cell-mediated cytotoxicity, complement-dependent cytotoxicity, antibody-dependent cell phagocytosis, antibody-dependent cytokine release, and cytokine release syndrome

For immune checkpoint inhibitors, Fc-mediated effector functions are undesirable and could even be detrimental.[11] For instance, ADCC and ADCP can deplete PD-1 expressing T cells and compromise the anti-tumor efficacy of anti-PD-1 antibodies,[12,13] so many antibody drugs targeting immune checkpoints, such as nivolumab choose to use IgG4 isotype to minimize Fc-induced effector functions. Fc-induced effector functions could also contribute to irAEs. For both safety and efficacy considerations, the Fc region of ivonescimab was engineered to carry the two mutations L234A and L235A (termed "DM") to reduce Fc–mediated immune effector functions. No measurable binding of ivonescimab to Fc gamma receptors and C1q was detected, while nivolumab showed binding to FcγRI and bevacizumab showed binding to all the Fc gamma receptors tested and C1q (Figure S5). Cellular assays were further conducted to confirm the functional consequences of Fc engineering. In ADCC assays, nivolumab displayed a dose-dependent ADCC activity in human PD-1 overexpressing CHO-K1 (CHO-K1-PD-1) cells, while ivonescimab exhibited no such activity (Figure 6A). As expected, neither nivolumab nor ivonescimab showed CDC activities against CHO-K1-PD-1 cells (Figure 6B). ADCP assays revealed that ivonescimab caused no apparent phagocytosis to CHO-K1-PD-1 cells, while nivolumab demonstrated robust ADCP activity (Figure 6C). ADCR assay also showed no IL-6 and IL-10 release for ivonescimab (Figure 6D). We further examined the effects of the Fc engineering of ivonescimab on inflammatory cytokine release on unstimulated PBMCs when incubated as a single agent. Ivonescimab did not elicit the secretion of IL-1β, TNF-α, or IL-6, while nivolumab triggered a strong release of these cytokines (Figure 6E). These findings together indicated that Fc engineering effectively eliminated FcγR-mediated effector functions of ivonescimab and remarkably abated inflammatory cytokine release from HPMMs, hinting a benign safety profile in terms of irAE occurrences.

Ivonescimab shows a favorable safety profile in non-human primates and clinical study

Since ivonescimab has cross-reactivity to cynomolgus monkey PD-1 and VEGF (Figure S6), the potential toxicity of ivonescimab was evaluated in mature cynomolgus monkeys (Table S1; Figure S7). No apparent toxicity was observed in cynomolgus monkeys after intravenous infusion of ivonescimab at a single dose of 100, 200, or 400 mg/kg. The maximum tolerated dose (MTD) was considered greater than or equal to 400 mg/kg. In a 4-week repeat-dose toxicity study, ivonescimab was clinically well tolerated by cynomolgus monkeys (5/gender/group) when administered intravenously once weekly at 10, 30, or 100 mg/kg following a 6-week recovery. No test article-related abnormal clinical observation was noted systemically or locally at the injection sites in animals, the exception being skin erythema at the whole body in one male monkey at 30 mg/kg. The highest non-severely toxic dose (HNSTD) for ivonescimab was 100 mg/kg under the given conditions.

Based on the overall results of preclinical studies, the safety and efficacy of ivonescimab are currently being evaluated in several clinical trials.[5,14] Hemorrhages, hypertension, proteinuria, and gastrointestinal perforation are the frequently reported adverse events in clinical studies of bevacizumab. We analyzed the incidence of these adverse events (Grade $\geq$3) in the clinical studies of ivonescimab. A total of 282 patients from 2 clinical trials (NCT04736823, NCT04900363)[5,6] were included in the analysis dataset. Grade $\geq$3 hemorrhages, hypertension, proteinuria, and gastrointestinal perforation occurred in 1%, 4.3%, 1.4%, and 0% of patients receiving ivonescimab, respectively, which were lower compared to that receiving bevacizumab (Table S2). Meanwhile, the incidents of irAE from these trials were assessed, and the number of selected safety events in ivonescimab was numerically lower relative to the published safety data of nivolumab (Table S3). In summary, these data suggest a favorable safety profile of ivonescimab.

DISCUSSION

Although antibodies targeting PD-1 or its ligand PD-L1 as immunotherapy have shown impressive clinical benefits in multiple tumor types, the relatively low response rate of anti-PD-1/PD-L1 therapy remains to be resolved. Bifunctional or bispecific antibodies containing anti-PD-1/PD-L1 moiety offer many exciting opportunities to simultaneously target different mechanisms that could be complimentary to the blockade of PD-1/PD-L1, such as the pathways that are involved in tumor angiogenesis for tumor development and immunosuppressive tumor microenvironment. Since VEGF not only drives angiogenesis and vascular permeability during tumorigenesis but also contributes to immunosuppressive effects by regulating various immune cells,[15] it is rational to design a single agent targeting both PD-1 and VEGF for cancer therapy. Several clinical trials involved in the combination of bevacizumab/ramucirumab and

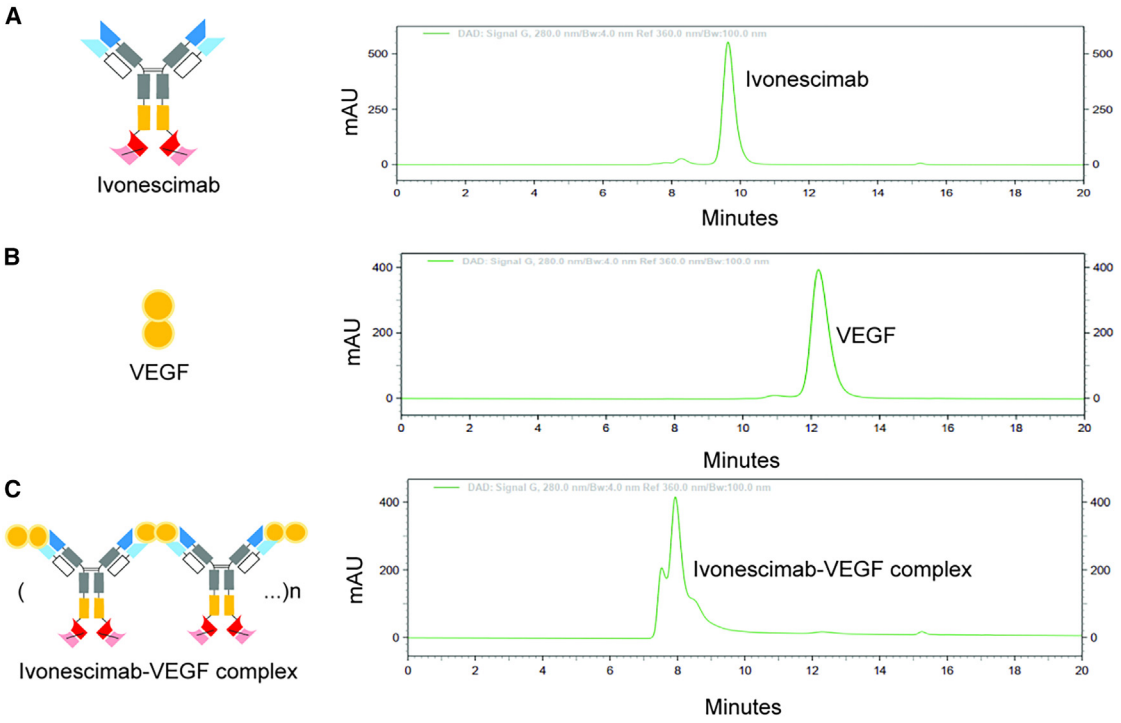

Figure 2. Ivonescimab forms soluble complexes with VEGF

(A–C) Ivonescimab alone (8 μM, A), VEGF alone (8 μM, B), or ivonescimab (8 μM) premixed with 2×VEGF (C) were analyzed on SEC-HPLC. Diagrams in the left panel represent ivonescimab, VEGF, and the proposed ivonescimab-VEGF complex structure. Also see Figure S1.

PD-1/PD-L1 inhibitors are ongoing and have shown promising clinical benefits.[16] Besides, as an alternative to combination therapy, several bispecific antibodies that target PD-1/L1 and VEGF are in development, such as PM8002,[17] HB0025,[18] IMM2510,[19] which are PD-L1/VEGF bispecific antibodies. However, most of these studies are still in the early stage of clinical development. And two PD-1/VEGF bispecific antibodies, JS207 and RC148, have entered the Phase I study recently.

Ivonescimab, a first-in-class tetravalent bispecific anti-VEGF/PD-1 antibody, is currently in multiple phase III global clinical trials for non-small cell lung cancer (NCT05184712, NCT05840016, and NCT05499390). In NSCLC trials, ivonescimab demonstrated surprisingly better clinical safety while maintaining efficacy relative to that observed for anti-PD-1/PD-L1 and bevacizumab combo. In particular, in patients with squamous non-small cell lung cancer where the use of bevacizumab is prohibited due to severe hemoptysis and other side effects, ivonescimab was well tolerated with minimal occurrence of hemoptysis and much reduced other typical side effects associated with bevacizumab, including hypertension.[4,5] Phase III trials of ivonescimab in squamous non-small cell lung cancer are underway. We believe the design features of ivonescimab afforded unique pharmacodynamic properties that distinguished ivonescimab from the combination use of anti-PD-1/PD-L1 and bevacizumab.

Compared to the combination therapy with two individual antibodies, one unique feature of bispecific antibodies is a potential increase of the binding and biological effect due to cooperative binding by two targets. This cooperativity can be achieved by simultaneously binding two multimerized target molecules. Ivonescimab, a tetravalent bispecific antibody with two binding sites for VEGF and two binding sites for PD-1, can bind both VEGF and PD-1 simultaneously (Figures 1A and 1B). In addition, VEGF exists naturally as a soluble homo-dimer. SEC data demonstrated that ivonescimab can form a soluble complex with VEGF, similar to the case of bevacizumab.[8,9] These protein complexes appeared to be a mixture with various numbers of ivonescimab molecules linked via VEGF dimers since our SEC data showed several high molecular weight peaks. In the tumor microenvironment, while abundant PD-1 and VEGF co-existing (Figure S8), we speculate that ivonescimab could form very stable "cluster" complexes with PD-1 and VEGF in which the binding of VEGF to ivonescimab strengthens its binding to PD-1 and vice versa (Figure 7). Indeed, we found that the antigen binding activity of ivonescimab to PD-1 was significantly enhanced in the presence of VEGF by 18-folds relative to penpulimab, and this is mainly due to the slower dissociation rate (Figure 3B). Likewise, PD-1 enhanced the binding affinity of ivonescimab to VEGF compared to the parental antibody bevacizumab (Figure 4B). This characteristic cooperative binding of ivonescimab suggested a novel mechanism of action that is distinct from the cases of using a combination of two antibodies targeting these two pathways, supported by our results that no cooperative binding of bevacizumab to VEGF and penpulimab to PD-1 were observed (Figures 7 and S2). To further support this concept, the cooperative binding of ivonescimab to VEGF and PD-1 leads to an increased functional valency of ivonescimab

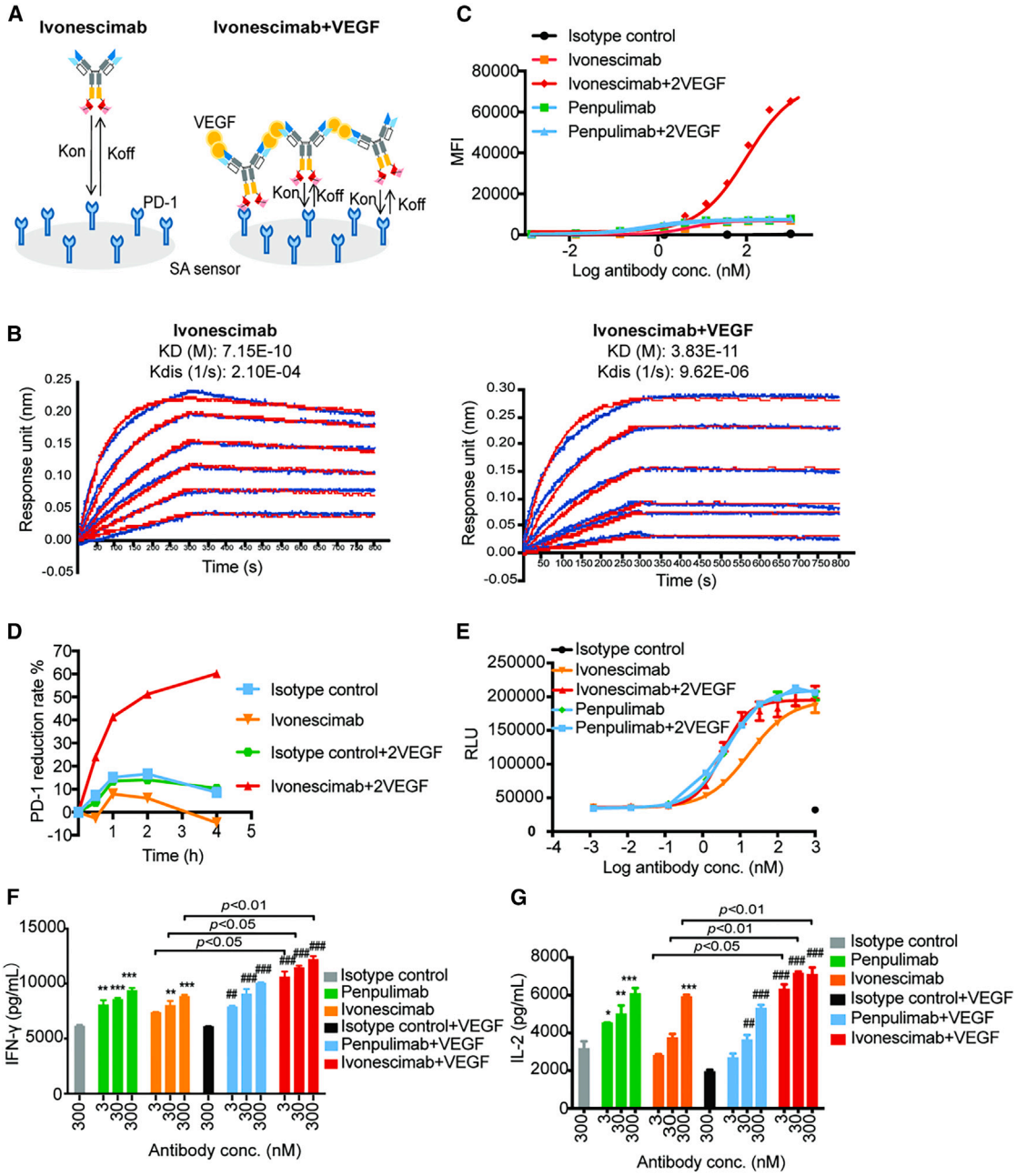

Figure 3. The presence of VEGF promotes binding avidity of ivonescimab to human PD-1 and facilitates better potency on the blockade of PD-1 signaling and T cell activation

(A) Diagram representing the binding profile of ivonescimab to PD-1 with or without VEGF.

(B) The binding kinetics of ivonescimab alone or ivonescimab-VEGF to immobilized PD-1-His-Biotin were determined by Fortebio Octet Molecular Interaction System. The binding kinetic parameters are shown above the sensorgram. Blue lines represent the real-time measurement of the binding affinity of ivonescimab with or without VEGF to PD-1, while red lines represent mathematical fitting curves based on blue lines.

(C) Binding of ivonescimab and anti-PD-1 antibody penpulimab with or without VEGF on PD-1 transfected Jurkat cells via FACS. MFI, mean fluorescent intensity.

(D) Cell surface PD-1 level on PD-1-expressing Jurkat cells, detected by FACS at different time points after ivonescimab incubation with or without VEGF. The reduction rates % were calculated from the decrease of surface PD-1 compared to its expression at 0 h.

(E) Ivonescimab and penpulimab with or without VEGF blocked the interaction of PD-1 and PD-L1, leading to the enhancement of luminescence in the co-culture of PD-L1 aAPC/CHO-K1 cells and PD-1 effector cells.

(F) IFN-γ and (G) IL-2 production in a mixed culture of hPBMCs and Raji-PD-L1 cells were analyzed by ELISA. Compared with the isotype control, $*p < 0.05$, $**p < 0.01$, $***p < 0.001$; compared with the isotype control+VEGF, $\#\#p < 0.01$, $\#\#\#p < 0.001$. Also see Figures S2 and S3.

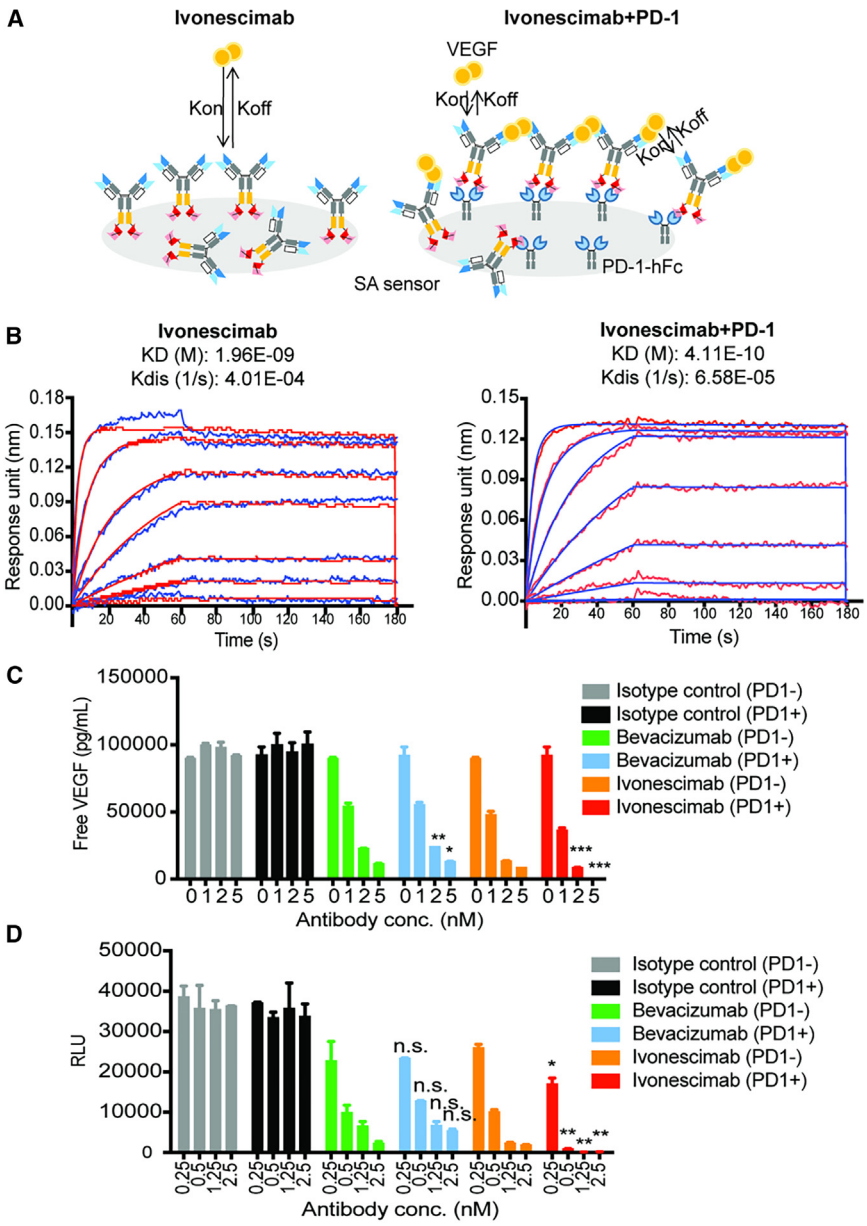

Figure 4. The presence of PD-1 promotes the binding avidity of ivonescimab to human VEGF and facilitates enhanced VEGF signaling blockade

(A) Diagram representing the binding profile of Ivonescimab to VEGF with or without PD-1.

(B) Ivonescimab (7 nM) alone (left) or a mixture of ivonescimab (7 nM) with PD-1-human Fc (PD-1-hFc, 7 nM) (right) were immobilized on the AHC sensor. The binding kinetics of the serial dilution of human VEGF-His protein (1000–1.37 nM) to immobilized ivonescimab or ivonescimab-PD-1-hFc were determined by Fortebio Octet Molecular Interaction System. The binding kinetic parameters were shown above the sensorgrams. Blue lines represent the real-time measurement of the binding affinity of ivonescimab with or without PD-1 to VEGF, while red lines represent mathematical fitting curves based on blue lines.

(C) Indicated antibodies were incubated with PD-1-His-Biotin-coated beads or control beads for 1 h in the presence of VEGF (5 nM). Then the supernatants without beads were measured for free VEGF by ELISA. Results of antibodies (PD-1+) were compared with the corresponding antibodies (PD-1-) group by t-test analysis, $^{*}p < 0.05$, $^{**}p < 0.01$, $^{***}p < 0.001$, n.s. is not significant.

(D) Luminescence signals in the 293T-KDR-NFAT-LUC cells treated with the same diluted supernatant in c as indicated were assessed by Steady-Glo Luciferase assay. Anti-HEL IgG1DM was used as an isotype control. Results of antibodies (PD-1+) were compared with the corresponding antibodies (PD-1-) group, $^{*}p < 0.05$, $^{**}p < 0.01$, $^{***}p < 0.001$ and n.s. represents no significance.

for both PD-1/L1 and VEGF signaling. VEGF and PD-1 are highly co-expressed within various human tumors (Figure S8). It is important to note that the greatest avidity of ivonescimab for PD-1 and VEGF will occur where the two targets are more likely to be found together and, therefore, may favor ivonescimab with increased retention in TME as opposed to the normal tissues of the body. We hypothesize that these properties have the potential to provide ivonescimab not only the augmented efficacy but also better safety.

A combination of anti-PD-1 with anti-VEGF inhibitors can be used as a strategy in cancer immunotherapy, but considerable adverse events are a predicament for the use of this regimen.[20] Toxicities including hemorrhages, hypertension, proteinuria, and gastrointestinal perforation, have been frequently announced in the clinical studies of bevacizumab,[21,22] and treatment of cancers with PD-1 inhibitors can lead to irAEs. Combined use of PD-1 inhibitors and VEGF blockers achieved some success but could lead to severe and even fetal adverse events in some cases.[23] The underlying mechanisms of its toxicities have not yet been fully characterized. One study suggested that bevacizumab may induce platelet activation and thrombosis by activating the platelet FcγRIIa receptor.[9] Also, irAEs are known to be related to the recruitment of immune cells carrying Fc receptors.[24–26] In contrast to most anti-PD-1 and anti-VEGF antibodies, which are IgG4 and IgG1 wild type, we introduced two mutations into the ivonescimab IgG1 Fc region to eliminate its Fc effector functions. In preclinical studies, we confirmed the lack of effector functions and the induction of proinflammatory cytokines by ivonescimab. In contrast, bevacizumab can bind to all Fc gamma receptors, and nivolumab showed FcγRI binding and can induce ADCC and ADCP.

Accumulating evidence indicated that combination therapy targeting different pathways can improve antitumor response. CD47 functions as a macrophage immune checkpoint by suppressing the activity of phagocytes through its interactions with

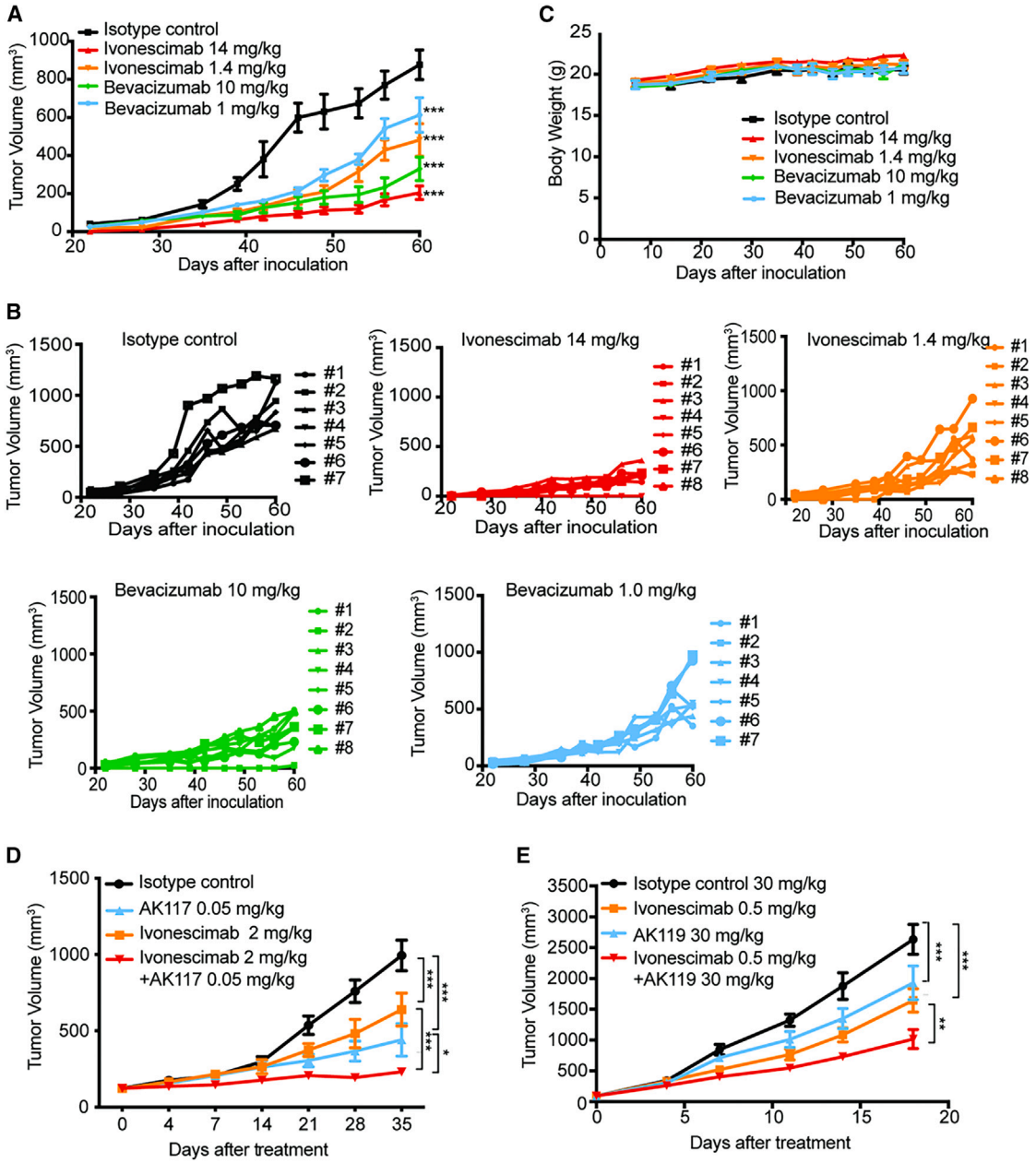

Figure 5. Ivonescimab demonstrates superior anti-tumor efficacy in both single/combination treatment in mice

(A–C) Each mouse was inoculated subcutaneously at the right hind flank with HCC827 cells, PBMCs, and ivonescimab, bevacizumab, or isotype control anti-HEL mixture on day 0. Different doses of antibodies were then continuously intravenously injected on day 7, 14, 21, 28, and 35. Tumor volume (A) and body weight (C) were measured (n = 7–8 for each group). (B) Spaghetti plots of all mice in each of the treatment groups are shown.

(D) MDA-MB-231 cells were subcutaneously inoculated in the SCID/Beige mice. Mice were grouped when tumor volume reached 120 mm^3 and intraperitoneally injected with activated hPBMCs. AK117 (anti-CD47 mAb) was then continuously intravenously injected twice per week for eight times and ivonescimab was administrated weekly for four times. Tumor volume was then monitored.

(E) MC38-hPD-L1/hCD73 cells were subcutaneously inoculated in the C57BL/6-hPD-1/hPD-L1/hCD73 transgenic mice. Mice were grouped when tumor volume reached 80–120 mm^3 and ivonescimab, AK119 (anti-CD73 mAb) or ivonescimab with AK119 were then intraperitoneally injected biweekly. Tumor volume was then monitored. $^*p < 0.05$, $^{**}p < 0.01$, $^{***}p < 0.001$. Comparisons of tumor growth among groups were analyzed using two-way ANOVA followed by Bonferroni's multiple comparison test. Also see Figure S4.

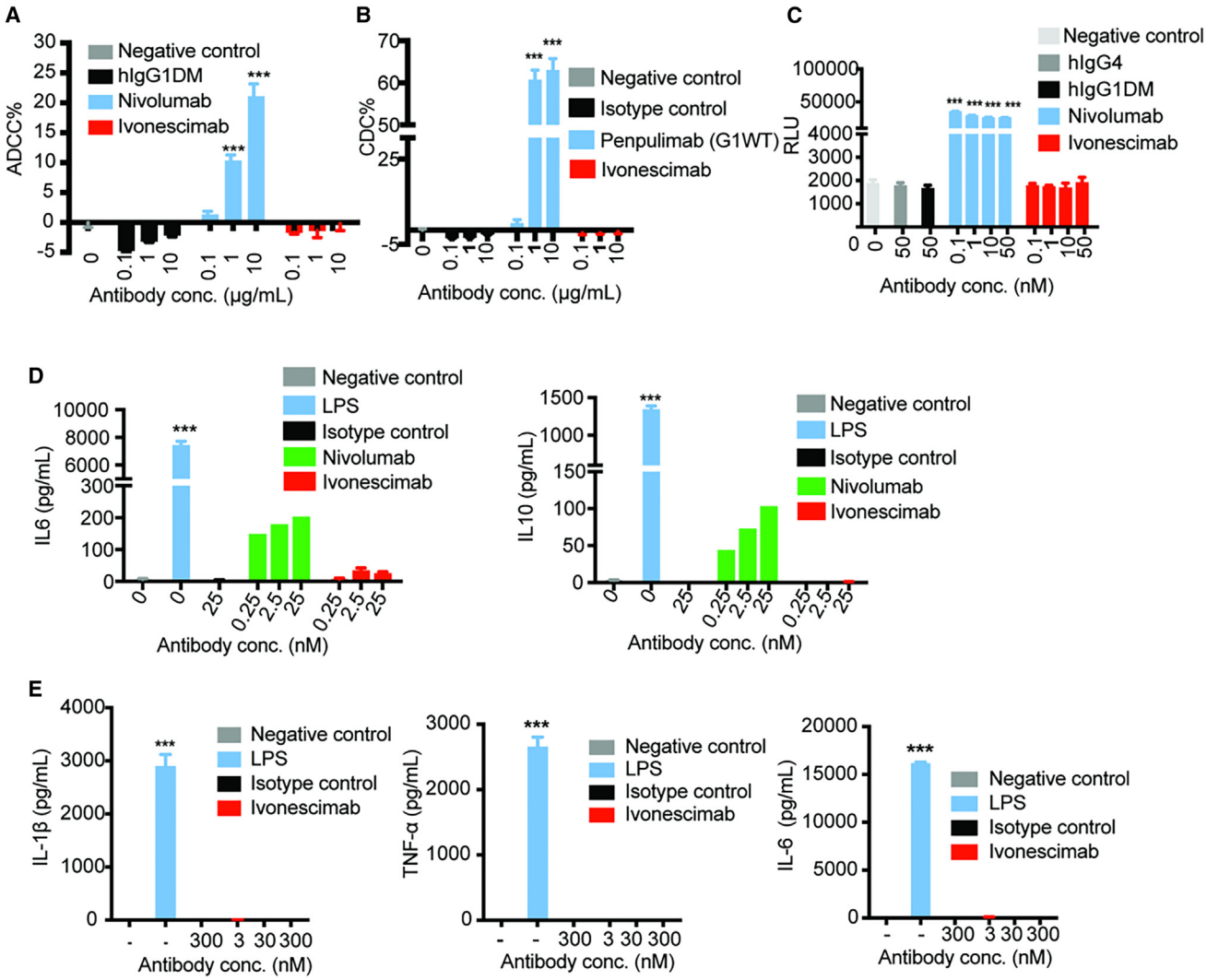

Figure 6. Favorable immunosafety profile of ivonescimab compared to nivolumab

(A) ADCC of ivonescimab was determined by measuring lactase dehydrogenase (LDH) release in the mixed culture of CHO-K1-PD-1 cells and human PBMCs.

(B) CDC of ivonescimab was determined by measuring LDH release from CHO-K1-PD-1 cells. The normal human serum complement was used as the source of complement.

(C) ADCP activities of ivonescimab were measured by reporter assay. Jurkat-NFAT-CD64^{-}CD32H cells and CHO-K1-PD-1 cells were cocultured for 5 h in the presence of indicated antibodies.

(D) IL-6 and IL-10 release by HPMMs cocultured with CHO-K1-PD-1 cells were examined by ELISA.

(E) The release of inflammatory cytokines IL-1β, TNF-α, and IL-6 from human PBMCs when treated with ivonescimab were assessed by ELISA. LPS was used as a positive control. Data are expressed as mean ± SEM and analyzed using one-way ANOVA. Compared with the negative control, ***$p < 0.001$. Also see Figure S5.

SIRPα on phagocytic cells, which gives a "do not eat me" signal to the innate immune system as a mechanism of immune escape. It is also reported that CD47 upregulation limits the antitumor effect of VEGF/VEGFR and PD-1/L1 inhibitors.[27] CD73 functions as an adenosinergic checkpoint by producing extracellular adenosine in TME, which not only inhibits antitumor T cell activity but also enhances the immune inhibitory function of cancer-associated fibroblasts and myeloid cells.[28] CD73 can also promote angiogenesis via the up-regulation of VEGF expression, which suggests that CD73 may contribute to acquired resistance to anti-VEGF therapy.[29] Thus, we believed that a combination treatment of ivonescimab with agents targeting these pathways may have a synergistic effect on antitumor activity. AK117 is an anti-CD47 antibody and AK119 is an anti-CD73 antibody developed by Akeso Biopharma. The combination treatment of ivonescimab with AK117 and AK119 was explored in this study, and the results showed that the antitumor efficacy was significantly improved. These results support our current clinical studies of ivonescimab in combination with AK117 (NCT05227664) and AK119 (NCT05636267).

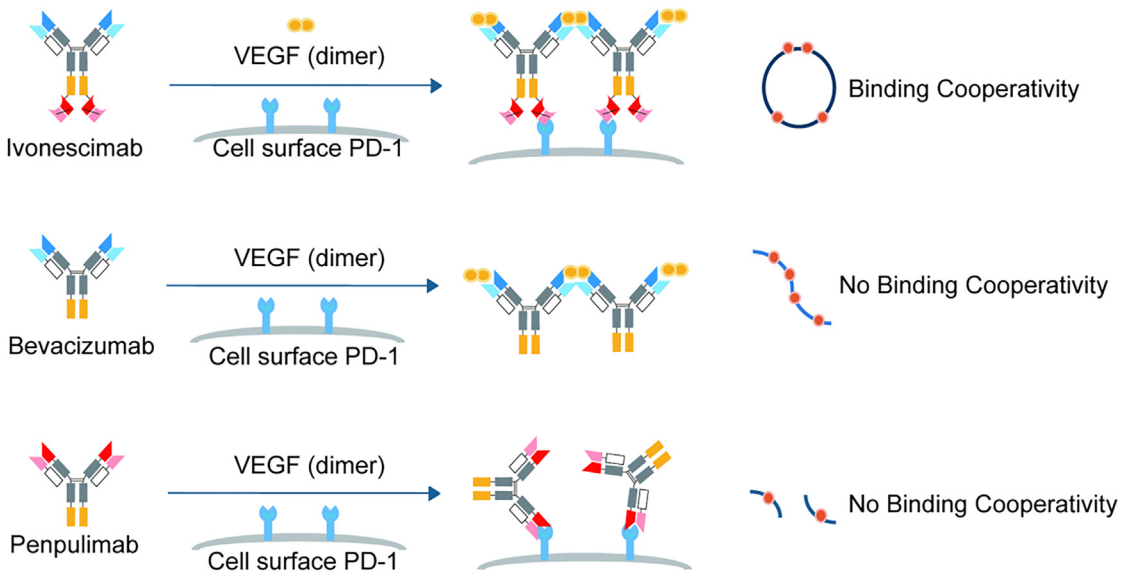

Figure 7. Model diagram of ivonescimab cooperative mechanisms of action

Conceptually, ivonescimab can bind with VEGF dimers and PD-1 simultaneously. When all 4 binding sites of ivonescimab are occupied by VEGF and PD-1 (top row), this "cluster" complex becomes the most stable structure in which the binding of VEGF to ivonescimab would strengthen its binding to PD-1, and vice versa. This propensity and interdependency type of interaction requiring the engagement of the tetravalent antibody and its two antigens is defined as cooperative binding. This complex structure is very stable and relevant to a mono-specific anti-VEGF antibody (such as bevacizumab, middle row) or an anti-PD-1 antibody (such as penpulimab, bottom row).

In conclusion, ivonescimab is a dual-blocking anti-PD-1/VEGF bispecific antibody with a symmetric tetravalent structure. Mechanistically, higher avidity to both PD-1 and VEGF by forming an ivonescimab-VEGF-PD-1 complex increased the cooperativity and functional valency of both PD-1 and VEGF signaling, coincident with robust anti-tumor activity in both mono- and combination study in mouse tumor models. In addition, the Fc engineering of ivonescimab eliminated its Fc effector functions including ADCC, CDC, and ADCP correlates with favorable safety results in clinical studies. Our findings established a solid foundation for ivonesicmab as a promising new therapeutic candidate, supporting its clinical development for the treatment of human cancers.

Limitations of the study

The limitations of this study include the need for a more mechanistic *in vivo* study. In this study, the unique cooperative binding of ivonescimab to its targets was observed *in vitro*, and the cooperative biological effects of ivonescimab on PD-1/L1 and VEGF signaling pathways were evaluated in cell-based *in vitro* assays. These findings, though mechanistically supporting, correlated with the improved efficacy and safety results of ivonescimab in the clinic. Further in-depth exploration of the *in vivo* cooperative effect by using humanized PD-1/PD-L1/VEGF triple knock-in mice could shed more light on the mechanism we mainly characterized *in vitro*.

RESOURCE AVAILABILITY

Lead contact

Further information and requests for resources and reagents should be directed to and will be fulfilled by the lead contact, Baiyong Li (baiyong.li@akesobio.com).

Materials availability

Plasmids and antibodies generated in this study will be available on request through the completion of a material transfer agreement.

Data and code availability

- All data reported in this article will be shared by the lead contact upon request.
- This article does not report the original code.
- Any additional information required to reanalyze the data reported in this article is available from the lead contact upon request.

ACKNOWLEDGMENTS

This study is all funded by Akeso Biopharma, and did not receive any specific grant from funding agencies in the public or not-for-profit sectors. The authors would like to thank all the colleagues contributed to this study.

AUTHOR CONTRIBUTIONS

Conceptualization, B.L. and M.X.; methodology and supervision, T.Z., Z.H., X.P., C.J., and W.L; investigation, J.D.; visualization, L.Z. and W.Y.; writing-original draft, B.L., J.M., L.Z., W.Y., and N.C., writing-review and editing, B.L., J.M., and L.Z.

DECLARATION OF INTERESTS

No potential conflicts of interest were disclosed by the authors.

STAR★METHODS

Detailed methods are provided in the online version of this paper and include the following:

- KEY RESOURCES TABLE
- EXPERIMENTAL MODEL AND STUDY PARTICIPANT DETAILS
  - Cell culture

SUPPLEMENTAL INFORMATION

Supplemental information can be found online at https://doi.org/10.1016/j.isci.2024.111722.

Received: January 2, 2024
Revised: May 8, 2024
Accepted: December 30, 2024
Published: December 31, 2024

REFERENCES

1. Carmeliet, P. (2005). VEGF as a key mediator of angiogenesis in cancer. Oncology *69*, 4–10. https://doi.org/10.1159/000088478.
2. Garcia, J., Hurwitz, H.I., Sandler, A.B., Miles, D., Coleman, R.L., Deurloo, R., and Chinot, O.L. (2020). Bevacizumab (Avastin®) in cancer treatment: A review of 15 years of clinical experience and future outlook. Cancer Treat Rev. *86*, 102017. https://doi.org/10.1016/j.ctrv.2020.102017.
3. Villaruz, L.C., and Socinski, M.A. (2015). The Role of Anti-angiogenesis in Non-small-cell Lung Cancer: an Update. Curr. Oncol. Rep. *17*, 26. https://doi.org/10.1007/s11912-015-0448-y.
4. Zhou, C., Ren, S., Luo, Y., Wang, L., Xiong, A., Su, C., Zhang, Z., Li, W., Zhou, J., Yu, X., et al. (2022). A phase Ib/II study of AK112, a PD-1/VEGF bispecific antibody, as first- or second-line therapy for advanced non–small cell lung cancer (NSCLC). J. Clin. Orthod. *40*, 9040. https://doi.org/10.1200/JCO.2022.40.16_suppl.9040.
5. Zhao, Y., Chen, G., Chen, J., Zhuang, L., Du, Y., Yu, Q., Zhuang, W., Zhao, Y., Zhou, M., Zhang, W., et al. (2023). AK112, a novel PD-1/VEGF bispecific antibody, in combination with chemotherapy in patients with advanced non-small cell lung cancer (NSCLC): an open-label, multicenter, phase II trial. eClinicalMedicine *62*, 102106. https://doi.org/10.1016/j.eclinm.2023.102106.
6. Wang, L., Luo, Y., Ren, S., Zhang, Z., Xiong, A., Su, C., Zhou, J., Yu, X., Hu, Y., Zhang, X., et al. (2024). A Phase 1b Study of Ivonescimab, a Programmed Cell Death Protein-1 and Vascular Endothelial Growth Factor Bispecific Antibody, as First- or Second-Line Therapy for Advanced or Metastatic Immunotherapy-Naive NSCLC. J. Thorac. Oncol. *19*, 465–475. https://doi.org/10.1016/j.jtho.2023.10.014.
7. Ohm, J.E., and Carbone, D.P. (2001). VEGF as a mediator of tumor-associated immunodeficiency. Immunol. Res. *23*, 263–272. https://doi.org/10.1385/IR:23:2-3:263.
8. MacDonald, D.A., Martin, J., Muthusamy, K.K., Luo, J.-K., Pyles, E., Rafique, A., Huang, T., Potocky, T., Liu, Y., Cao, J., et al. (2016). Aflibercept exhibits VEGF binding stoichiometry distinct from bevacizumab and does not support formation of immune-like complexes. Angiogenesis *19*, 389–406. https://doi.org/10.1007/s10456-016-9515-8.
9. Meyer, T., Robles-Carrillo, L., Robson, T., Langer, F., Desai, H., Davila, M., Amaya, M., Francis, J.L., and Amirkhosravi, A. (2009). Bevacizumab immune complexes activate platelets and induce thrombosis in FCGR2A transgenic mice. J. Thromb. Haemostasis *7*, 171–181. https://doi.org/10.1111/j.1538-7836.2008.03212.x.
10. Buchbinder, E.I., and Desai, A. (2016). CTLA-4 and PD-1 pathways: similarities, differences, and implications of their inhibition. Am. J. Clin. Oncol. *39*, 98–106. https://doi.org/10.1097/COC.0000000000000239.
11. Wang, X., Mathieu, M., and Brezski, R.J. (2018). IgG Fc engineering to modulate antibody effector functions. Protein Cell *9*, 63–73. https://doi.org/10.1007/s13238-017-0473-8.
12. Arlauckas, S.P., Garris, C.S., Kohler, R.H., Kitaoka, M., Cuccarese, M.F., Yang, K.S., Miller, M.A., Carlson, J.C., Freeman, G.J., Anthony, R.M., et al. (2017). In vivo imaging reveals a tumor-associated macrophage-mediated resistance pathway in anti-PD-1 therapy. Sci. Transl. Med. *9*, eaal3604. https://doi.org/10.1126/scitranslmed.aal3604.
13. Moreno-Vicente, J., Willoughby, J.E., Taylor, M.C., Booth, S.G., English, V.L., Williams, E.L., Penfold, C.A., Mockridge, C.I., Inzhelevskaya, T., Kim, J., et al. (2022). Fc-null anti-PD-1 monoclonal antibodies deliver optimal checkpoint blockade in diverse immune environments. J. Immunother. Cancer *10*, e003735. https://doi.org/10.1136/jitc-2021-003735.
14. Zhang, L., Fang, W., Zhao, Y., Yang, Y., Zhou, N., Chen, L., Huang, Y., Chen, J., Zhuang, L., Du, Y., et al. (2023). Phase II results of ivonescimab (AK112/SMT112), a novel PD-1/VEGF bispecific, in combination with chemotherapy for first line treatment of advanced or metastatic non-small cell lung cancer (NSCLC) without actionable genomic alterations (AGA) in EGFR/ALK. J. Clin. Oncol. *41*, 9087. https://doi.org/10.1200/JCO.2023.41.16_suppl.9087.
15. Goel, H.L., and Mercurio, A.M. (2013). VEGF targets the tumour cell. Nat. Rev. Cancer *13*, 871–882. https://doi.org/10.1038/nrc3627.
16. Gao, F., and Yang, C. (2020). Anti-VEGF/VEGFR2 Monoclonal Antibodies and their Combinations with PD-1/PD-L1 Inhibitors in Clinic. Curr. Cancer Drug Targets *20*, 3–18. https://doi.org/10.2174/1568009619666191114110359.
17. Guo, Y., Guo, J., Cheng, Y., Wang, Z., Li, Y., Lv, D., Yin, Y., Li, G., Wu, L., Huang, Y., et al. (2023). Phase Ib/IIa Safety and Efficacy of PM8002, a Bispecific Antibody Targeting PD-L1 and VEGF-A, as a Monotherapy in Patients with Advanced Solid Tumors. Am Soc. Clin. Oncol. *41*, 2536. https://doi.org/10.1200/JCO.2023.41.16_suppl.2536.
18. Cui, X., Jia, H., Xin, H., Zhang, L., Chen, S., Xia, S., Li, X., Xu, W., Chen, X., Feng, Y., et al. (2021). A Novel Bispecific Antibody Targeting PD-L1 and VEGF With Combined Anti-Tumor Activities. Front. Immunol. *12*, 778978. https://doi.org/10.3389/fimmu.2021.778978.
19. Cheng, X., Song, Z., Zhang, J., Jin, J., Gao, S., Liu, R., Sun, Y., Zhang, Y., Gao, S., Jia, R., et al. (2023). Preliminary Results of a Phase I Dose Escalation Study of IMM2510, a PD-L1 and VEGF Bispecific Fusion Protein, in Patients with Advanced Tumors. Am Soc. Clin. Oncol. *41*, 2535. https://doi.org/10.1200/JCO.2023.41.16_suppl.2535.
20. Gu, T., Jiang, A., Zhou, C., Lin, A., Cheng, Q., Liu, Z., Zhang, J., and Luo, P. (2023). Adverse reactions associated with immune checkpoint inhibitors and bevacizumab: A pharmacovigilance analysis. Int. J. Cancer *152*, 480–495. https://doi.org/10.1002/ijc.34332.
21. Marín-Pozo, J.F., Duarte-Pérez, J.M., and Sánchez-Rovira, P. (2016). Safety, Effectiveness, and Costs of Bevacizumab-Based Therapy in

Southern Spain: A Real World Experience. Medicine *95*, e3623. https://doi.org/10.1097/MD.0000000000003623.

22. Dang, A., Jagan Mohan Venkateswara Rao, P., Kishore, R., and Vallish, B.N. (2021). Real world safety of bevacizumab in cancer patients: A systematic literature review of case reports. Int. J. Risk Saf. Med. *32*, 163–173. https://doi.org/10.3233/JRS-194051.

23. Conroy, M., and Naidoo, J. (2022). Immune-related adverse events and the balancing act of immunotherapy. Nat. Commun. *13*, 392. https://doi.org/10.1038/s41467-022-27960-2.

24. Bauché, D., Mauze, S., Kochel, C., Grein, J., Sawant, A., Zybina, Y., Blumenschein, W., Yang, P., Annamalai, L., Yearley, J.H., et al. (2020). Antitumor efficacy of combined CTLA4/PD-1 blockade without intestinal inflammation is achieved by elimination of FcγR interactions. J. Immunother. Cancer *8*, e001584. https://doi.org/10.1136/jitc-2020-001584.

25. Occhipinti, M., Falcone, R., Onesti, C.E., and Marchetti, P. (2018). Hyperprogressive Disease and Early Hypereosinophilia After Anti-PD-1 Treatment: A Case Report. Drug Saf. Case Rep. *5*, 12. https://doi.org/10.1007/s40800-018-0078-z.

26. Jodai, T., Yoshida, C., Sato, R., Kakiuchi, Y., Sato, N., Iyama, S., Kimura, T., Saruwatari, K., Saeki, S., Ichiyasu, H., et al. (2019). A potential mechanism of the onset of acute eosinophilic pneumonia triggered by an anti-PD-1 immune checkpoint antibody in a lung cancer patient. Immun. Inflamm. Dis. *7*, 3–6. https://doi.org/10.1002/iid3.238.

27. Zhang, X., Wang, Y., Fan, J., Chen, W., Luan, J., Mei, X., Wang, S., Li, Y., Ye, L., Li, S., et al. (2019). Blocking CD47 efficiently potentiated therapeutic effects of anti-angiogenic therapy in non-small cell lung cancer. J. Immunother. Cancer *7*, 346. https://doi.org/10.1186/s40425-019-0812-9.

28. Kurago, Z., Guo, G., Shi, H., Bollag, R.J., Groves, M.W., Byrd, J.K., and Cui, Y. (2023). Inhibitors of the CD73-adenosinergic checkpoint as promising combinatory agents for conventional and advanced cancer immunotherapy. Front. Immunol. *14*, 1212209. https://doi.org/10.3389/fimmu.2023.1212209.

29. Gao, Z.w., Dong, K., and Zhang, H.z. (2014). The Roles of CD73 in Cancer. BioMed Res. Int. *2014*, e460654. https://doi.org/10.1155/2014/460654.

30. Huang, Z., Pang, X., Zhong, T., Qu, T., Chen, N., Ma, S., He, X., Xia, D., Wang, M., Xia, M., and Li, B. (2022). Penpulimab, an Fc-Engineered IgG1 Anti-PD-1 Antibody, With Improved Efficacy and Low Incidence of Immune-Related Adverse Events. Front. Immunol. *13*.

31. Qu, T., Zhong, T., Pang, X., Huang, Z., Jin, C., Wang, Z.M., Li, B., and Xia, Y. (2022). Ligufalimab, a novel anti-CD47 antibody with no hemagglutination demonstrates both monotherapy and combo antitumor activity. J. Immunother. Cancer *10*, e005517. https://doi.org/10.1136/jitc-2022-005517.

STAR★METHODS

KEY RESOURCES TABLE

REAGENT or RESOURCE	SOURCE	IDENTIFIER
Antibodies		
Ivonescimab	Akeso Biopharma	N/A
Penpulimab	Akeso Biopharma	N/A
Bevacizumab	Akeso Biopharma	N/A
Nivolumab	Akeso Biopharma	N/A
IgG1DM isotype control	Akeso Biopharma	N/A
AK117	Akeso Biopharma	N/A
AK119	Akeso Biopharma	N/A
Human IgG1 (anti-HEL)	Akeso Biopharma	N/A
Rabbit anti-PD1 antibody	Sino Biological	Cat# 10377-R002; RRID:AB_2860161
Alexa Fluor™ 488 goat anti-rabbit IgG (H+L) antibody	Thermo Fisher Scientific	Cat# A-11008; RRID:AB_143165
Biological samples		
PBMCs	Zhongshan provincial blood center	N/A
HPMMs	Akeso Biopharma	N/A
Chemicals, peptides, and recombinant proteins		
Bovine Serum Albumin (BSA)	Sigma	V900933-1KG, B2064-100G
Goat anti-human IgG (H+L)-HRP	Jackson	109-035-088
Fetal bovine serum, FBS	Jackson	109-095-098
Tetramethyl benzidine (TMB) color development substrate	Neogen	308177
Fetal bovine serum (FBS)	Gibco	10270-106
Sulfo-NHS-LC Biotinylation	Thermo	21335
Zeba desalting spin columns	Thermo	89882
Trypsin-EDTA	Gibco	25300-054
Hygromycin B	Invitrogen	10687010
Puromycin	Amresco	J593-25MG
Antibiotic G-418 Sulfate Solution	Gibco	11811-23
Sodium pyruvate	Gibco	11360-070
MEM nonessential amino acids	Gibco	11140-050
0.25% Trypsin-EDTA	Gibco	25200
0.05% Trypsin-EDTA	Gibco	25300-054
CCK8	Amresco	298-93-1
SEB (staphylococcal enterotoxin B)	Toxin technology	BT202
MMC (mitomycin C)	Stressmarq	SIH-246
FcγRI-his	Sino Biological	LAC11AP1710
FcγRIIIa-Biotin	Sino Biological	10389-H27H1-B
C1q	Fitzgerald	32R-AC049
Human PD1-mFc	Akeso Biopharma	N/A
Human PD1-hFc	Akeso Biopharma	N/A
Human PD1-His-Biotin	Akeso Biopharma	N/A
Human VEGF-His	Akeso Biopharma	N/A
VEGFR2-mFc-Bio	Akeso Biopharma	N/A
Critical commercial assays		
Bright-Glo™ Luciferase Assay System	Promega	2620, G7940

(*Continued on next page*)

Continued

REAGENT or RESOURCE	SOURCE	IDENTIFIER
LDH assay kit	Roche	11644793001
ELISA	Dakewe	1110202,1110002
DynabeadsTM M280 anti-mouse IgG Fc beads	Thermofisher	11202D
Experimental models: Organisms/strains		
SCID/Beige mice	Beiing Vital River Laboratory AnimalTechnology Co., Ltd.	N/A
C57BL/6-hPD-1/hPD-L1/hCD73 transgenic mice	GemPharmatech Co., Ltd	N/A
Cynomolgus monkeys (M. fascicularis)	Guangxi Guidong Quadrumana Development&Laboratory Co. Ltd. (Guigang, Guangxi, CHN) Guangxi Grandforest Scientific Primate Company (Guigang, Guangxi, CHN), Ltd. Beijing Primas Biotech Co. Ltd. (Beijing, CHN)	N/A
Experimental models: Cell lines		
293T cells	Wuhan University	N/A
293T-PD1 cells	Akeso Biopharma	N/A
Jurkat cells	Chinese Academy of Sciences	SCSP-513
Jurkat-PD-1 cells	Akeso Biopharma	N/A
HUVECs	Allcells	H-001F-C
PD-L1 aAPC/CHO-K1 cells	Promega	J112A
PD-1 effector cells	Promega	J108A
293T-KDR-NFAT-LUC cells	Akeso Biopharma	N/A
Raji cells	Chinese Academy of Sciences, Shanghai Branch	TCHu 44
Raji-PD-L1 cells	Akeso Biopharma	N/A
Jurkat-NFAT-CD64-CD32H cells	Akeso Biopharma	N/A
HCC827	JENNIO Biological	N/A
MDA-MB-231	ATCC	N/A
MC38-hPD-L1/hCD73 cells	GemPharmatech	N/A
CHO-K1-PD-1 cells	Akeso Biopharma	N/A
Software and algorithms		
Fortebio Octet molecular interaction system	Pall/Fortebio	Model: Octet QKe
Fortebio Data Acquisition 7.0		N/A
Fortebio Data Analysis 7.0		N/A
Ficoll-Paque^{TM} Plus	GE	17-1440-02
Prism 8.0	GraphPad	https://www.graphpad.com/feature
FlowJo_V10	BD Biosciences	https://www.flowjo.com/

EXPERIMENTAL MODEL AND STUDY PARTICIPANT DETAILS

Cell culture

HUVECs (human umbilical vein endothelial cell) were cultured in HUVEC cell culture medium (Allcells, H-004). 293T cells were cultured in DMEM with 10% FBS. Jurkat cells were cultured in RPMI 1640 with 10% fetal bovine serum (FBS). The culture conditions were maintained at 37°C in a 5% CO2 incubator of humidified. Human peripheral blood were obtained from Zhongshan Blood Center and donated by female/male healthy volunteers. All the volunteers have assigned informed consent statement. Then human peripheral blood mononuclear cells (hPBMCs) were isolated using Ficoll-Paque^{TM} Plus (GE, 17-1440-02). Human peripheral monocyte-derived macrophages (HPMMs) were differentiated from hPBMCs.

Mouse experiments

Female or male SCID/Beige mice were purchased from Beijing Vital River Laboratory Animal Technology Co., Ltd. Both animal studies were reviewed and approved by Akeso Biopharma Animal Experiment Ethics Committee, and the ethical approval number are 20180928-01 and 20210506-01 respectively; C57BL/6-hPD-1/hPD-L1/hCD73 transgenic mice were purchased from Gempharmatech Co., Ltd. All animals were housed in a specific pathogen-free environment with free access to food and water. The animal study was reviewed and approved by Institutional Animal Care and Use Committee (IACUC) of Gempharmatech Co., Ltd, and the ethical approval number is GPTAP20211122-4.

Monkey experiments

Cynomolgus monkeys (*M. fascicularis*) of Mauritian origin were obtained from Guangxi Guidong Quadrumana Development&Laboratory Co. Ltd. (Guigang, Guangxi, CHN), Guangxi Grandforest Scientific Primate Company (Guigang, Guangxi, CHN), Ltd. and Beijing Primas Biotech Co. Ltd. (Beijing, CHN). Male and female monkeys (3 to 4.5 years old) were randomly assigned by algorithm to study groups (Beijing, CHN). Monkeys were housed under appropriate environmental (temperature, humidity, light cycle) conditions and were offered purified and chlorinated tap water *ad libitum* and fed Diet Certified commercial monkey diet (Keaoxieli) with a daily ration of fruits. The study procedures were approved by the Institutional Animal Care and Use Committee, and the ethical approval number is AUC21-2419.

METHOD DETAILS

Antibodies

Ivonescimab, a humanized symmetrical bispecific antibody targeting both human PD-1 and VEGF, has an IgG-scFv format. Briefly, to construct the bispecific antibody, we fused the scFv of anti-PD-1 onto the C terminus of the heavy chain of anti-VEGF antibody via a flexible (Gly4Ser) linker. Ivonescimab has a heterotetrameric structure consisting of two heavy chains of the IgG1 subclass and two light chains of the kappa subclass, which are covalently linked through disulfide bonds. Mutations (L235A/L236A termed DM) were introduced into the Fc region to eliminate binding to FcγRs and C1q. IgG1DM isotype control was generated by introducing L235A/L236A mutations into the Fc region of a human IgG1. Research-grade nivolumab (anti-PD-1 by BMS) and bevacizumab (anti-VEGF by Roche) were produced in-house according to the published sequences. AK117, AK119 and penpulimab (Akeso Biopharma) were also constructed in-house as described.[30,31] All drug substances are produced in Chinese hamster ovary (CHO) cells using recombinant DNA technology. Purified proteins were detected by conventional SDS-PAGE and SEC-HPLC analytical methods.

Enzyme-linked immunosorbent assay (ELISA)

ELISA was used to detect the binding activities of ivonescimab, nivolumab and bevacizumab to human PD-1-mFc and human VEGF-His. Fusion protein of mouse Fc with human PD-1 extracellular domain (PD-1-mFc, 0.5 μg/mL) or human 6× histidine-tagged VEGF (VEGF-His, 1 μg/mL) was coated onto a 96-well microplate overnight at 4°C. The antigen-coated microplate was washed with PBST (phosphate-buffered saline with Tween 20) and then blocked with blocking buffer (1% BSA in PBST) at 37°C for 2 hours. Serial dilutions (1:3) of ivonescimab and nivolumab starting at 0.333 μg/mL or ivonescimab and bevacizumab starting at 1 μg/mL were prepared and added into the microplate for incubation at 37°C for 30 minutes, and then washed with PBST for 3 times. The washed microplate was incubated with goat anti-human IgG (H+L)-HRP (1:5000; Jackson, 109-035-088) at 37°C for 30 minutes, and then washed with PBST for 3 times. Tetramethyl benzidime (TMB) was added into the microplate and developed in darkness for 5 minutes. The reaction was stopped by adding 2 M H_2SO_4. All samples were treated in duplicate. The absorbance value was read in a Molecular Devices reader at 450 nm and analyzed with SoftMax Pro 6.2.1.

ELISA competitive binding

To determine the competition acitvity of ivonescimab and human PD-L1 to human PD-1, ivonescimab and human VEGFR to human VEGF respectively, human PD1-hFc (0.5 μg/mL) or human VEGF-His (2.0 μg/mL) was coated onto a 96-well microplate and incubated at 4°C overnight. The antigen-coated microplate was washed with PBST and then blocked with blocking buffer (1% BSA in PBST) at 37°C for 2 hours. Serial dilutions (1:3) of ivonescimab and nivolumab or bevacizumab starting at 10 μg/mL were prepared and added into the microplate to generate a 7-point response curve. Human PD-L1-mFc (0.6 μg/mL) or human VEGFR2-mFc-bio (0.2 μg/mL) was also added to the microplates respectively and incubated for 30 minutes. After washing with PBST for 3 times, the goat anti-mouse IgG-HRP (1:5000) was added and incubated at 37°C for 30 minutes, the microplate was washed with PBST for 4 times. TMB was added and developed in darkness for 5 minutes. The reaction was stopped by adding 2 M H_2SO_4. All samples were treated in duplicate. The microplate was read in a Molecular Devices reader at a wave length of 450 nm and analyzed with SoftMax Pro 6.2.1 to create a Four Parameter Logistic (4PL) curve fit by plotting the antibody concentration on x-axis and OD on y-axis.

Antibody internalization by microscopic imaging

Antibody internalization over time were tracked by confocal microscopy. Brifly, 293T-PD-1 cells were preincubated with antibodies (300 nM) which premixed with PE anti-human IgG Fc antibody at 4°C for 30 minutes in the presence of VEGF (600 nM) or not. After

washing to remove excess antibodies (time zero), cells were incubated at 37°C to initiate internalization and imaged by microscopy at indicated time point. Antibody internalization was also quantified as intracellular spot PE sum intensity mean per well and divided by total antibody intensity to determine % IgG internalized by image J.

Flow cytometry binding assay

Cell binding activities were determined on human PD-1 transfected 293T (293T-PD-1) cells. Briefly, 293T-PD-1 cells were washed with PBSA (PBS with 1% BSA) and incubated with 3-fold serial dilution of antibodies for 30 minutes at 4°C. To detect the cell binding of antibodies in the presence of VEGF, antibodies were premixed with VEGF at molar ratios of 1:2. Human IgG1 was set as isotype control. After washing with PBSA, cell-bound antibodies were detected with anti-human IgG secondary antibody. The analysis was performed using Becton Dickinson FACS Calibur. MFI (mean fluorescence intensity) values of samples were analyzed using FlowJo software.

Binding kinetic analysis by BLI

Bio-Layer Interferometry (BLI) was performed by Fortebio Octet Qke or Fortebio Octet red96e. To detect binding activity of ivonescimab to human PD-1 and human VEGF simultaneously, PBST was used as buffer solution and ivonescimab (20 μg/mL) was immobilized on the surface of AR2G sensor by amine coupling. Human PD-1 (PD-1-hFc, 5 μg/mL) and then human VEGF (VEGF-his, 5 μg/mL) were flowed over the chip surface sequentially or in reverse order, buffer were used as blank control. To measure the affinity of antibodies to human VEGF, antibody alone or antibody with PD-1 protein (preincubated at molar ratio of 1:1) or were immobilized on the AHC sensor and 3-fold serial dilution of VEGF-His (1000 nM to 1.37 nM) was flowed over the sensor chip. To measure the affinity of antibodies to human PD-1, human PD1-His-biotin (200 nM) were immobilized on the SA sensor or not, and 2-fold serial dilution of antibodies alone or antibody with VEGF (preincubated at molar ratio of 1:1) were flowed over the sensor chip. To determine the affinity to C1q, the antibodies (300 nM) were immobilized onto FAB2G sensor. Two-fold serial dilution of C1q (10 nM to 0.625 nM) was then flowed over the chip surface. To determine the affinity to FcγRI and FcγRIIIa, FcγRI (1 μg/mL) and FcγRIIIa (5 μg/mL) were immobilized on the HIS1K sensor, respectively, and 2-fold serially diluted antibody (50 nM to 3.12 nM for FcγRI, 200 nM to 12.5 nM for FcγRIIIa) was flowed through the chip. To determine the affinity to human PD-1, biotinylated fusion protein of human Fc with human PD-1 extracellular domain (PD-1-hFc-Bio) or biotinylated histidine-tagged PD-1 (PD-1-His-Bio) was immobilized on SA sensors, and 2-fold serial dilution of ivonescimab, ivonescimab-VEGF complex (preincubated at molar ratio of 1:1) or nivolumab (50 nM to 3.1 nM) was flowed over the sensor chip. The data was collected using Fortebio data Acquisition 7.0 or 12.0 and analyzed using Fortebio Data Analysis 12.0 or Fortebio Data Analysis 7.0 or HT12.0.

Reporter gene assay

For PD-1/PD-L1 blockade reporter gene assay, PD-L1 aAPC/CHO-K1 cells (CHO-K1 cells stably expressing human PD-L1 and a cell surface protein designed to activate cognate TCRs in an antigen-independent manner, Promega, J112A) and PD-1 effector cells (Jurkat cells stably expressing human PD-1 and NFAT-induced luciferase, Promega, J108A) were used. The presence of anti-PD-1/L1 antibodies can block the PD-1/PD-L1signal pathway, activate Jurkat cells and induce NFAT-dependent luciferase expression. On the day before the assay, PD-L1 aAPC/CHO-K1 cells were harvested and seeded into 96-well plates at 40,000 cells per well in Ham's F-12 with 10% FBS. On the assay day, the culture medium in the assay plates was replaced with assay medium (1640 medium containing 1% heat-inactivated FBS), and PD-1 effector cells were then added at 5×10^4 cells per well. Serial dilution of antibodies ranging from 400 nM to 0.0067 nM was added into the assay plates and incubated for 5-6 hours. Human IgG1 was used as an isotype control and tested at 400 nM. Specifically, to measure the PD-1/PD-L1 blockade by antibodies with or without VEGF, ivonescimab or penpulimab was premixed with VEGF or not at molar ratio of 1:2 and then diluted at 3-fold from 1000 nM to 0.00123 nM. After incubation, Bio-Glo™ Reagent (Promega, E2650) was then added and incubated for 5-30 minutes. The luminescence was quantified using Envision multimode plate reader.

For VEGF responsive reporter gene assay, 293T-KDR-NFAT-LUC (293T cells expressing NFAT response element upstream of luciferase as well as exogenous human vascular endothelial growth factor receptor 2 (also named kinase insert domain receptor, KDR)) stable cell line was constructed and validated by FACS. Briefly, VEGF (30 ng/ml) alone or VEGF preincubated with different dilution of antibodies was added into the assay plates pre-seeded with 293T-KDR-NFAT-LUC and incubated for 4 hours. Promega Bright-Glo™ Luciferase Assay reagent (Promega, E2650) was then added and incubated at room temperature for 5 minutes. Relative Light Unit (RLU) was determined by Envision multimode plate reader.

HUVEC proliferation assay

HUVEC proliferation in response to VEGF and the inhibitory effect of antibodies was measured by CCK8 assay. Briefly, HUVECs (3,000 cells/well) were seeded into 96-well plates and incubated overnight. The culture medium was replaced with assay medium (RPMI 1640 containing 2% heat inactivated FBS). VEGF (20 nM) with or without serially diluted antibodies were subsequently added and incubated for 3 days followed by adding of 2 μL CCK-8 reagent (Amresco, 0793-500MG) and incubating for 2 hours. The optical density (OD) values at 450-490 nm were quantified using Molecular Devices PLUS384 micro-plate reader.

Size-exclusion high-pressure liquid chromatography (SEC-HPLC)

The amounts of high molecular weight species (HMWS) present in ivonescimab alone, human VEGF alone or mixed samples of ivonescimab and human VEGF (molar ratio of 1:2) were analyzed by SEC using TSKgel G3000SWXL column (Tosoh Corp, 7.8 mm I.D.× 30 cm). The mobile phase was consisted of 50 mM sodium phosphate dibasic dodecahydrate, 628 mM sodium chloride, 13.5 mM potassium chloride and 10 mM monobasic potassium phosphate. The experimental conditions were as follows: flow rate: 0.8 mL/min; column temperature: ambient; sample temperature: ambient; run time: 20 minutes; detection wavelength: 280 nm; injection protein: 20 μg.

Cell surface PD-1 reduction assay

Ivonescimab-mediated PD-1 reduction on cell surface was determined on Jurkat-PD-1 cells with or without VEGF. Jurkat-PD-1 (6×10^5 cells/well) were pretreated with ivonescimab (300 nM) or ivonescimab-VEGF mixture (molar ratio=1:2) for 1 hour on ice. IgG1DM with or without VEGF was used as control. Cells were then washed and further incubated at 37°C for 0, 0.5, 1, 2, 4 hours. Following the incubation, cells were washed with PBSA and incubated with non-competing rabbit anti-PD1 antibody (Sino Biological, 10377-R002) for 1 hour on ice. Then, cells were stained with Alexa Fluor™ 488 goat anti-rabbit IgG (H+L) antibody (Thermofisher, A-11008) in the dark on ice for 30 minutes. After washing, the analysis was performed by FACS. MFI values of samples were acquired using FlowJo software. The reduction rates % were calculated from the decrease of cell surface PD-1 level compared to its expression at 0 hour.

Mixed lymphocyte reaction (MLR) assay

Human PBMCs were stimulated with 0.5 μg/mL staphylococcal enterotoxin B (SEB, Toxin technology, BT202) for 2 days in 37°C and 5% CO2 incubator. Raji-PD-L1 cells were treated with 2 μg/mL Mitomycin C (MMC, Stressmarq, SIH-246) for 1 hour in an incubator. Meanwhile, various concentration of antibodies was pre-incubated with human VEGF (500 ng/mL) at 37°C for 30 minutes. The SEB-stimulated PBMCs and MMC-treated Raji-PD-L1 cells were harvested and then seeded into 96-well plates at 1.0×10^5 cells/well. Antibodies or antibodies with VEGF were subsequently added into the plates containing cells and incubated for 72 hours. Three days later, the supernatants were then harvested for the measurement of IL-2 and IFN-γ by ELISA (Dakewe, 1110202, 1110002). Human IgG1DM was setup as an isotype control.

Depletion of VEGF assay

The ability of antibody to deplete VEGF in the presence or absence of PD-1 was evaluated in an *in vitro* system described in the following. First, various concentrations of testing antibodies were incubated with 5 nM VEGF, the mAb (monoclonal antibody)-VEGF mixtures were then incubated for 1.5 hours in a 96-well plate with Dynabeads™ M-280 anti-mouse IgG Fc beads (Thermofisher, 11202D) coated with high concentration of PD-1-mFc protein to model high PD-1 expression in the TME. The mAb-VEGF mixtures incubated with Dynabeads™ M-280 anti-mouse IgG Fc beads alone served as a PD-1-negative (PD-1-) control. Following the incubation, the remaining free VEGF in the supernatants were measured by a sandwich ELISA. Briefly, the free VEGF was captured by an ivonescimab/bevacizumab competitive binding VEGF antibody and then was detected by biotinylated anti-VEGF antibody/SA-HRP.

ADCC assay

ADCC activities were determined by measuring lactase dehydrogenase (LDH) release from the target cells. PBMCs from a healthy volunteer were isolated using Ficoll-Paque™ Plus (GE, 17-1440-02). CHO-K1-PD-1 cells plated in 96-well plate (3×10^4 cells per well) were incubated with serially diluted ivonescimab, nivolumab or isotype control for 1 hour at room temperature and then incubated with 9×10^5 PBMCs at 37°C for 4 hours. Thereafter, the LDH release in the supernatant was measured by LDH assay kit (Roche, 11644793001). ADCC activity was reported as percentage of LDH release and calculated as follows: ADCC% = ((OD of the experimental group - OD of the negative control group)/(OD of the positive control group - OD of the negative control group)) × 100%.

CDC assay

CDC activities were determined by measuring LDH release from cells. The normal human serum complement purchased from Quidel was used as the source of complements. CHO-K1-PD-1 cells plated in 96-well plate (3×10^4 cells per well) were incubated with serially diluted ivonescimab, nivolumab or isotype control for 10 minutes at room temperature. Thereafter, normal human serum complement at the final concentration of 2% was added and incubated at 37°C for 4 hours. Then the LDH release was measured as described above. CDC activity was reported as percentage of LDH release and calculated as follows: CDC% = ((OD of the experimental group - OD of the negative control group)/(OD of the positive control group - OD of the negative control group)) × 100%.

ADCP assay

ADCP activities were determined by reporter gene assay. Jurkat-NFAT-CD64-CD32H cells (constructed by Akeso Biopharma) which stably expressing FcγRI (CD64), FcγRIIa (CD32a) and luciferase driven by NFAT response elements were used as effector cells, and CHO-K1-PD-1 cells were used as target cells. Jurkat-NFAT-CD64-CD32H cells and CHO-K1-PD-1 cells were seeded into 96-well

plates at 4×10^4 cells per well and cocultured with antibodies for 5 hours. After incubation, Promega Bright-Glo™ Luciferase Assay reagent was then added, and incubated at room temperature for 5 minutes. The luminescence was quantified by Envision multimode plate reader.

ADCR assay

Human peripheral blood-derived monocytes were differentiated into macrophages (HPMMs) in 1640-CM (RPMI 1640 medium plus 10% FBS) containing human M-CSF (Peprotech, 300–25) for 7 days in a 37°C incubator with 5% CO_2. IFN-γ at 50 ng/ml (Sinobiological, 11725-HNAS-100) was added for the final 24 hours of the differentiation. HPMMs were collected and seeded into 96-well plates for further 24 hours of culture. CHO-K1-PD-1 cells were then co-cultured with HPMMs plus indicated antibodies in an incubator for 24 hours. LPS (Sigma, Cat.: L4391) was set as a positive control. Following the incubation, the supernatants were harvested for measurement of IL-8 and IL-6 using ELISA kits (Dakewe, 1110802, 1110602) according to the instructions.

Cytokine release from unstimulated PBMCs

Cytokine release was analyzed *in vitro* by using unstimulated PBMCs. Briefly, 200,000 PBMCs were seeded in each well of a 96-well plate and incubated with indicated concentrations of antibodies at 37°C in incubator. 24 hours later, the supernatants were collected and IL-1β, IL-6 and TNF-α were detected by ELISA kits (Dakewe, 1110122, 1110602, 1117202). LPS at 100 ng/mL was used as a positive control.

Murine tumor model

For monotherapy study, 5-7 weeks female SCID/Beige mice (Beijing Vital River Laboratory Animal Technology) were divided into five groups with 7-8 mice per group. PBMCs were stimulated with staphylococcal enterotoxin B (SEB, 0.2 μg/mL) for 72 hours. Mice were inoculated subcutaneously at the right hind flank with mixture of 6×10^6 HCC827, 8×10^5 PBMCs and indicated dose of antibody at day 0. Then the indicated antibodies were continuously intravenously injected on day 7, 14, 21, 28, and 35. In this model, PBMCs were mixed with HCC827 cells to provide immune component that is responsive to antibody blocking PD-1and generate anti-tumor immune response.

Two combination therapy studies of ivonescimab were also performed. Anti-tumor activity of ivonescimab combo with AK117 was evaluated in a humanized PD-1 mouse mode. MDA-MB-231 cells were subcutaneously inoculated in the SCID/Beige mice. Mice were grouped when tumor volume reached 120 mm^3 and intraperitoneally injected with activated hPBMCs. AK117 was then continuously intravenously injected twice per week for eight times and ivonescimab was administrated weekly for four times. Anti-tumor activity of ivonescimab combo with AK119 was test in the C57BL/6-hPD-1/hPD-L1/hCD73 transgenic mice which subcutaneously inoculated with MC38-hPDL1/hCD73 cells. Mice were grouped when tumor volume reached 80-120 mm^3 and indicated antibodies were then intraperitoneally injected biweekly.

The tumor volume (TV) was measured every 3 days and calculated according to the formula $TV = 0.5*a*b^2$, where a refers to the major diameter of the tumor, b refers to the short diameter of the tumor.

Toxicity studies in the cynomolgus monkey model

For single dose and 4-week toxicity studies, male and female cynomolgus monkeys (*M. fascicularis*, 3 to 4.5 years old) were randomly grouped and dosed intravenously as described in the table. Clinical observations, ophthalmoscopy, body weights, body temperature, electrocardiogram, hematology, coagulation, and clinical chemistry were performed on all monkeys and the data were reviewed by a veterinarian before being transferred from the holding colony. Clinical observations, body weights, body temperature were measured every week. Blood samples were drawn from a peripheral vein every 2 weeks for hemotological analysis. Hematology, coagulation, and clinical chemistry were performed at the end of study on all monkeys.

QUANTIFICATION AND STATISTICAL ANALYSIS

Statistical analyses

Statistical analyses were performed using one-way ANOVA, two-way ANOVA followed by Bonferroni's multiple comparison test (*in vivo* experiment) or T-test analysis with Prism version 7 software (GraphPad Software, Inc., La Jolla, CA). Data were expressed as number and percentage (%) or mean ± standard error of mean (SEM), and $p < 0.05$ was considered statistically different.

ADDITIONAL RESOURCES

Clinical trial registry numbers

The incidence of immune-related adverse events in the clinical studies of ivonescimab were obtained from 2 clinical trials: NCT04736823 and NCT04900363 (web links are provided below), and the data cut-off date is November 15th, 2022.

NCT04736823: https://clinicaltrials.gov/study/NCT04736823?term=NCT04736823&rank=1.

NCT04900363: https://clinicaltrials.gov/study/NCT04900363?term=NCT04900363&rank=1.